© 2016 IJSRST | Volume 2 | Issue 5 | Print ISSN: 2395-6011 | Online ISSN: 2395-602X
Themed Section: Science and Technology

On the Formation of Solid Solutions with Blödite- and Kröhnkite-Type Structures. I. Synthesis, Vibrational and EPR Spectroscopic Investigations of $Na_2Zn_{1-x}Cu_x(SO_4)_2{\cdot}4H_2O$ ($0 < x < 0.14$)

M. Georgiev[1], Tsv. Bancheva[1], D. Marinova[2], R. Stoyanova[2], D. Stoilova[2*]

[1]Department of Inorganic Chemistry, University of Chemical Technology and Metallurgy, 1756 Sofia, Bulgaria
*[2]Institute of General and Inorganic Chemistry, Bulgarian Academy of Sciences, 1113 Sofia, Bulgaria

ABSTRACT

The solubility diagram of the $Na_2Zn(SO_4)_2$–$Na_2Cu(SO_4)_2$–H_2O system at 25 ºC reveals that the copper ions are incorporated in the crystals of blödite-type structure, thus forming solid solutions of the type $Na_2Zn_{1-x}Cu_x(SO_4)_2{\cdot}4H_2O$ ($0 < x < 0.14$). However, the zinc cations do not accept the coordination environment of the copper ions in the strongly distorted CuO_6 octahedra (effect of Jahn-Teller) and as a consequence $Na_2Cu(SO_4)_2{\cdot}2H_2O$ free of zinc ions crystallizes in a wide concentration range.

Infrared spectra of the double salts, $Na_2Zn(SO_4)_2{\cdot}4H_2O$ and $Na_2Cu(SO_4)_2{\cdot}2H_2O$, as well as those of the solid solutions are presented and discussed with respect to the normal vibrations of the sulfate ions and water motions. The experimental results show that new bands corresponding to ν_3 of sulfate ions appear in the spectra of the solid solutions due to the new bands Cu–OSO_3. The strength of the hydrogen bonds as deduced from the frequencies of ν_{OH} and ν_{OD} of matrix-isolated HDO molecules (spectral range of 2500–2200 cm^{-1}) is discussed and the influence of the metal–water interactions (*synergetic* effect) on the hydrogen bond strength in both double sulfates is commented. The water librations are also briefly discussed.

The EPR spectra of $Na_2Cu(SO_4)_2{\cdot}2H_2O$ and $Na_2Zn_{1-x}Cu_x(SO_4)_2{\cdot}4H_2O$ are presented and discussed with respect to the crystal sites of the Cu^{2+} cations. The EPR measurements confirm the claim that the Zn cations are not incorporated in the crystals of the kröhnkite-type structure.

Keywords : $Na_2Zn_{1-x}Cu_x(SO_4)_2$ $4H_2O$ solid solutions; Solubility diagram; Vibrational spectra; Hydrogen bond strength; EPR spectra.

I. INTRODUCTION

The great interest of the scientists towards double sodium sulfates having 3d-transition metals is determined by their promising electrochemical properties. For example, the perspective of using blödite-type compounds $Na_2M(SO_4)_2{\cdot}4H_2O$ (M = Mg, Fe, Co, Ni, Zn) as a new type of insertion electrodes is described in detail in Refs. [1,2]. The sodium ion batteries are considered as an alternative to the lithium ion batteries owing to the lower price of sodium as compared to that of lithium.

Recently, two of the authors (D.M. and R.S) have reported experimental results of the electrochemical activity of manganese-based sulfate of alluaudite-type structure prepared from $Na_2Mn(SO_4)_2{\cdot}2H_2O$ (kröhnkite-type structure). The authors commented that alluaudite phase $Na_{2+\delta}Mn_2{}_{-\delta/2}(SO_4)_3$ displays a better electrochemical performance in comparison to that of well-known lithium manganese phospho-olivine $LiMnPO_4$ [3].

The blödite-type compounds $Na_2M(SO_4)_2{\cdot}4H_2O$ (M = Mg, Fe, Co, Ni, Zn) crystallize in the monoclinic SG $P2_1/a$ [4-8]. The crystal structures of these compounds are built up from isolated $[M(H_2O)_4(SO_4)_2]^{2-}$ clusters, which are interlinked by distorted NaO_6 polyhedra and hydrogen bonds. The NaO_6 octahedra are linked two by two through edges, thus forming isolated Na_2O_{10} bi-octahedra. The ionic transport properties of the blödite-type compounds are favored by the sodium ions which sit in the large channels running along the [100] direction. All atoms, except the divalent metal ions, which lie at center of inversion C_i, are located at general positions C_1. Two crystallographically different water molecules exist in the structure, which form hydrogen bonds of medium strength (the four bond distances Ow···O vary in the interval of 2.704–2.926 Å). In a previous paper of one of the authors the strength of the hydrogen bonds in the above compounds as deduced from the frequencies of ν_{OD} of matrix-isolated HDO molecules is discussed [8]. It has been established that the strength of the hydrogen bonds increases on going from the magnesium salt to the zinc one due to the increasing covalency of the respective M–OH_2 bonds (Mg < Co < Ni < Zn).

$Na_2Cu(SO_4)_2{\cdot}2H_2O$ belongs to a large number of natural and synthetic compounds built up of kröhnkite-type octahedral-tetrahedral chains. M. Fleck *at all*. have reviewed the structures of these compounds and presented a classification scheme for compounds with kröhnkite-type octahedral-tetrahedral chains [9,10]. The copper compound crystallizes in the monoclinic SG $P2_1/c$ (structural type D). The structure is composed of $CuO_4(H_2O)_2$ octahedra alternating with each two SO_4 tetrahedra by sharing corners. The chains are linked by Na cations (sodium ions form NaO_7 polyhedra) and hydrogen bonds, thus forming layers. These layers are then linked by hydrogen bonds and Na cations to a 3D structure. The SO_4 tetrahedra act as polydentate ligands – they are involved in metal–oxygen bonds including Na and Cu cations, but only two oxygen atoms from the tetrahedra are coordinated to Cu cations. The $CuO_4(H_2O)_2$ octahedra are strongly distorted as a result of the Jahn-Teller effect. The copper ions occupy C_i site symmetry and are linked to the water molecules via the shortest bonds (bond length Cu–OH_2 is 1.937 Å; bond distances Ow···O1 and Ow···O4 have values of 2.626 and 2.699 Å) [11]. $Na_2Cu(SO_4)_2{\cdot}2H_2O$ is reported to form the strongest hydrogen bonds among the sodium sulfates with kröhnkite-type octahedral-tetrahedral chains due to the strong M–OH_2 interactions (strong *synergetic* effect) [12]. The crystal structures of the zinc and copper compounds are shown in Fig. 1.

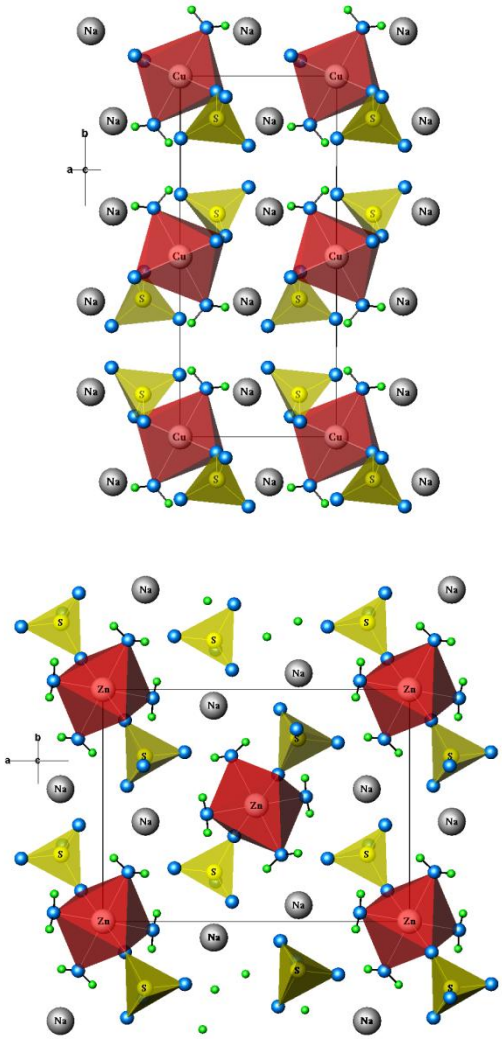

Figure 1: Crystal structures of: $Na_2Cu(SO_4)_2\ 2H_2O$ (up) and $Na_2Zn(SO_4)_2\ 4H_2O$ (down) in a projection along the *c*-axis

The current paper is a part of our plan to study the possibility for the formation of solid solutions of double sulfate crystal hydrates of blödite- and kröhnkite-type structure, on one hand, and on the other – solid solutions of anhydrous salts. For the first time experimental results on the preparation and characterization of solid solutions between sodium zinc sulfate tetrahydrate and sodium copper sulfate dihydrate are provided. In order to investigate the crystallization processes in mixed sodium zinc and copper solutions we studied the solubility diagram of the $Na_2Zn(SO_4)$–$Na_2Cu(SO_4)_2$–H_2O system at 25 ºC using the method of isothermal decrease of supersaturation. As a first step of our study we reported the results of spectroscopic investigations (IR, Raman and EPR) of both the neat double sulfates and the solid solutions.

II. METHODS AND MATERIAL

The double salts $Na_2Zn(SO_4)_2 \cdot 4H_2O$ and $Na_2Cu(SO_4)_2 \cdot 2H_2O$ were obtained by crystallization from ternary solutions according to the solubility diagrams of the three-component Na_2SO_4–$Cu(Zn)SO_4$–H_2O systems at 25 ºC [13]. The crystals were filtered, washed with ethanol and dried in air. The crystallization process in the ternary system $Na_2Zn(SO_4)_2$–$Na_2Cu(SO_4)_2$–H_2O was studied using the method of isothermal decrease of supersaturation described in Ref. [14]. Solutions containing different ratios of the salt components were heated at about 60-70°C (transparent solutions were obtained) and then cooled to 25 ºC. The saturated solutions were vigorously stirred for two days in order to reach the equilibrium between the solid and liquid phases. The analysis of the liquid and wet solid phases was performed, as follows: the sum of the metal ions (Zn and Cu) was determined complexonometrically at pH 5.5-6 using xylenol orange as indicator; the copper ion concentration was determined iodometrically; the concentration of the sodium zinc sulfate was calculated by difference. The content of the salt components in the completely dry solid phases were calculated using the method of algebraic indirect identification of the solid phase compositions [15].

The infrared spectra were recorded on a Nicolet iS5 Fourier transform interferometer (resolution < 2 cm^{-1}) at ambient temperature. The spectra were obtained using KBr discs as matrices. Ion exchange or other reactions with KBr have not been observed (infrared spectra using Nujol mulls were also measured). In some cases Lorentz band profile for multi peak data was used to determine the correct band positions (ORIGIN PRO 6.1). The Raman spectra were recorded with a Horiba Jobin-Yvon LabRAM HR800 spectrometer using 600 1/mm grating and a 633 nm He-Ne laser line for excitation. The samples were placed under the 50x achromatic objective of a Olympus BX41 microscope and measured in back scattering configuration. The laser power on the sample was kept bellow 5.54 mW so that no heating and dehydration effects on the powder sample could be observed.

The EPR spectra of the powder samples were recorded as the first derivative of the absorption signal of a Bruker EMX^{plus} EPR spectrometer in the X-band (9.4 GHz) within the temperature range of 120-450 K. The relative EPR intensity was determined by double integration of the signal, registered in the form of the first derivative. The spectra were simulated by using the program SIMFONIA (Bruker).

III. RESULTS AND DISCUSSION

A. Crystallization processes in the $Na_2Zn(SO_4)_2$–$Na_2Cu(SO_4)_2$–H_2O system at 25 ºC

The solubility diagram of the above system is shown in Fig. 2 (see also Table 1). The solubility curve consists of two branches, thus indicating the formation of two type of solid phases – solid solutions $Na_2Zn_{1-x}Cu_x(SO_4)_2 \cdot 4H_2O$ ($0 < x < 0.14$) formed on the basis of isodimorphous substitution of zinc cations by copper ones and $Na_2Cu(SO_4)_2 \cdot 2H_2O$. The experiments reveal that the crystals of $Na_2Zn(SO_4)_2 \cdot 4H_2O$ includes up to 14 mol% of copper ions (the formation of the above solid solutions is proved also by X-ray powder diffraction; the results will be published in a forthcoming paper). $Na_2Cu(SO_4)_2 \cdot 2H_2O$ free of zinc ions crystallizes in a wide concentration range – from the binary saturated solution of the sodium copper sulfate up to solutions containing 25.27 mass% sodium zinc sulfate and 10.00 mass% sodium copper sulfate. The concentrations of the double salts in their saturated binary solutions determined by analysing the solutions have values of: 32.25 mass% sodium zinc sulfate and 27.15 mass% sodium copper sulfate (calculated as anhydrous salts).

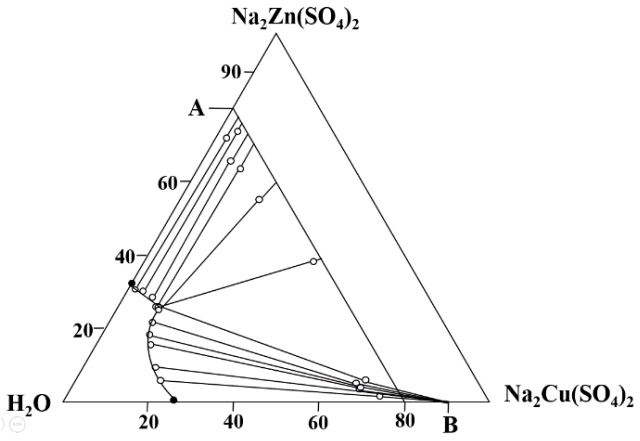

Figure 2: Solubility diagram of the $Na_2Zn(SO_4)_2$–$Na_2Cu(SO_4)_2$–H_2O system at 25 ºC (A, B, points corresponding to $Na_2Zn(SO_4)_2 \cdot 4H_2O$ and $Na_2Cu(SO_4)_2 \cdot 2H_2O$, respectively

According to the classical rules solid solutions are generally formed when the guest ions are able to accept the coordination environment of the host ions and the

TABLE I
SOLUBILITY IN THE $Na_2Zn(SO_4)_2$–$Na_2Cu(SO_4)_2$–H_2O SYSTEM AT 25 °C

Liquid phase, mass%		Wet solid phase, mass%		Composition of the solid phases
NaZnS	**NaCuS**	**NaZnS**	**NaCuS**	
32.25	-	-	-	$Na_2Zn(SO_4)_2\ 4H_2O$
31.05	1.75	71.50	2.30	$Na_2Zn_{0.97}Cu_{0.03}(SO_4)_2\ 4H_2O$
30.29	3.61	74.84	4.04	$Na_2Zn_{0.95}Cu_{0.05}(SO_4)_2\ 4H_2O$
28.50	7.58	66.04	7.14	$Na_2Zn_{0.92}Cu_{0.08}(SO_4)_2\ 4H_2O$
26.30	9.41	64.54	10.63	$Na_2Zn_{0.86}Cu_{0.14}(SO_4)_2\ 4H_2O$
25.27	10.00	54.90	18.67	euthonics
26.50	9.90	38.74	40.17	"-"
27.74	10.64	6.62	69.57	$Na_2Cu(SO_4)_2\ 2H_2O$
22.14	11.09	6.50	66.56	- " -
17.83	12.31	4.82	66.76	- " -
16.24	14.50	4.50	69.57	- " -
9.86	17.21	"-"	"-"	- " -
5.97	20.66	2.21	74.08	- " -
-	27.15	-	-	- " -

host salt retains its lattice. The formation of the neat sodium copper sulfate free of zinc ions means that these ions could not replace the copper ions in the kröhnkite structure due to the strong deformation of the copper octahedra as a result of the Jahn-Teller effect.

It is worth mentioning that the isodimorphous substitution of zinc ions by copper ions in the orthorhombic $ZnSO_4{\cdot}7H_2O$ more than 2 mol% leads to a change in the structure of the host compounds – monoclinic solid solutions are formed in the concentration interval of 16 mol% up to 34 mol% of copper ions (this phenomenon is observed also and for $MgSO_4{\cdot}7H_2O$) [16]). According to the authors the transformation of the orthorhombic lattices into monoclinic ones is owing to the distortion of the octahedra $Zn(Mg)O_6$ with respect to the Zn(Mg)–O bond lengths caused by the included Jahn-Teller copper ions.

However, in the case of $Na_2Zn(SO_4)_2{\cdot}4H_2O$ containing copper guest ions such a change in the blödite-type structure does not occur (see Fig. 2) due probably to the buffer effect of the sodium ions and the hydrogen bonds, which undertake the strain in the lattice caused by the guest copper ions. However, when the concentration of copper ions included in the crystals of $Na_2Zn(SO_4)_2{\cdot}4H_2O$ increases more than 14 mol% the cooperative Jahn-Teller effect results in the interruption in the series of the solid solutions, this leading to the crystallization of $Na_2Cu(SO_4)_2{\cdot}2H_2O$.

B. Infrared spectroscopic study of the neat sulfates and of solid solutions $Na_2Zn_{1-x}Cu_x(SO_4)_2{\cdot}4H_2O$

1) Factor group analysis:

Four internal vibrations characterize the free tetrahedral ions (XO_4^{n-}) under perfect T_d symmetry: $\nu_1(A_1)$, the symmetric X–O stretching modes, $\nu_2(E)$, the symmetric XO_4 bending modes, $\nu_3(F_2)$ and $\nu_4(F_2)$, the asymmetric stretching and bending modes, respectively. The normal vibrations of the free sulfate ions in aqueous solutions are reported to appear, as follows: $\nu_1 = 983\ cm^{-1}$, $\nu_2 = 450\ cm^{-1}$, $\nu_3 = 1105\ cm^{-1}$, $\nu_4 = 611\ cm^{-1}$ [17].

The monoclinic unit cell of $Na_2Zn(SO_4)_2{\cdot}4H_2O$ (Z = 2; factor group symmetry C_{2h}) contains 50 atoms with 150 zone-center degrees of freedom.

The SO_4^{2-} ions (four SO_4^{2-} ions in the unit cell located on C_1 sites) and the water molecules (eight molecules in the unit cell located on C_1 sites) contribute 60 internal modes to the 150 optical zone-center modes (each tetrahedral ions is characterized with nine normal vibrations and each water molecule with three normal vibrations, i.e. 36 internal modes for the tetrahedral ions and 24 internal modes for the water molecules). The static field (related to the low symmetry C_1 of the sites on which the SO_4^{2-} ions are situated) will cause a removal of the degeneracy of

both the doubly degenerate ν_2 modes and the triply degenerate ν_3 and ν_4 modes (the non-degenerate ν_1 mode is activated). The nine internal modes of the tetrahedral ions are of A symmetry as predicted from the site group analysis: one mode for the symmetric stretching vibrations (ν_1), two modes for the symmetric bending vibrations (ν_2), and three modes for both asymmetric stretching and bending vibrations (ν_3 and ν_4). Additionally, under the factor group symmetry C_{2h} each species of A symmetry split into four components – Ag + Bg + Au + Bu (related to interactions of identical oscillators, correlation field effect, see Fig.3). Consequently, the 36 optical modes for the SO_4^{2-} ions are subdivided into 9Ag + 9Bg + 9Au + 9Bu modes. As was mentioned above the water molecules contribute 24 modes, as follows – 6Ag + 6Bg + 6Au + 6Bu.

The remaining 87 optical modes (external modes) are distributed between the translational and librational lattice modes. Thus, the unit cell theoretical treatment for the translational (Na^+, SO_4^{2-}, $H_2O(1)$, and $H_2O(2)$ – all in C_1 site symmetry, Zn^{2+} – in C_i site symmetry) and librational lattice modes (SO_4^{2-}, $H_2O(1)$, and $H_2O(2)$) yields: 51 translations (12Ag + 12Bg + 14Au + 13Bu) and 36 librations (9Ag + 9Bg + 9Au + 9Bu).

Then the 150 vibrational modes of the unit cell decompose according to the following representation:

Γ = 36Ag + 36Bg + 39Au + 39Bu; where 1Au + 2Bu are translations (acoustic modes).

$Na_2Cu(SO_4)_2{\cdot}2H_2O$ crystallizes also in the monoclinic space group (Z = 2; factor group symmetry C_{2h}) with 38 atoms in the unit cell with 114 zone-center degrees of freedom. The SO_4^{2-} ions (four SO_4^{2-} ions in the unit cell located on C_1 sites) and the water molecules (four molecules in the unit cell located on C_1 sites) contribute 48 internal modes to the 114 optical zone-center modes – 36 internal modes for the tetrahedral ions and 12 internal modes for the water molecules). The remaining 63 optical modes are distributed between the translational and librational lattice modes, as follows: 42 translations for (Na^+, SO_4^{2-}, H_2O – all in C_1 site symmetry, Cu^{2+} – in C_i site symmetry; 9Ag + 9Bg + 12Au + 12Bu) and 24 librations (SO_4^{2-} and H_2O; 6Ag + 6Bg + 6Au + 6Bu).

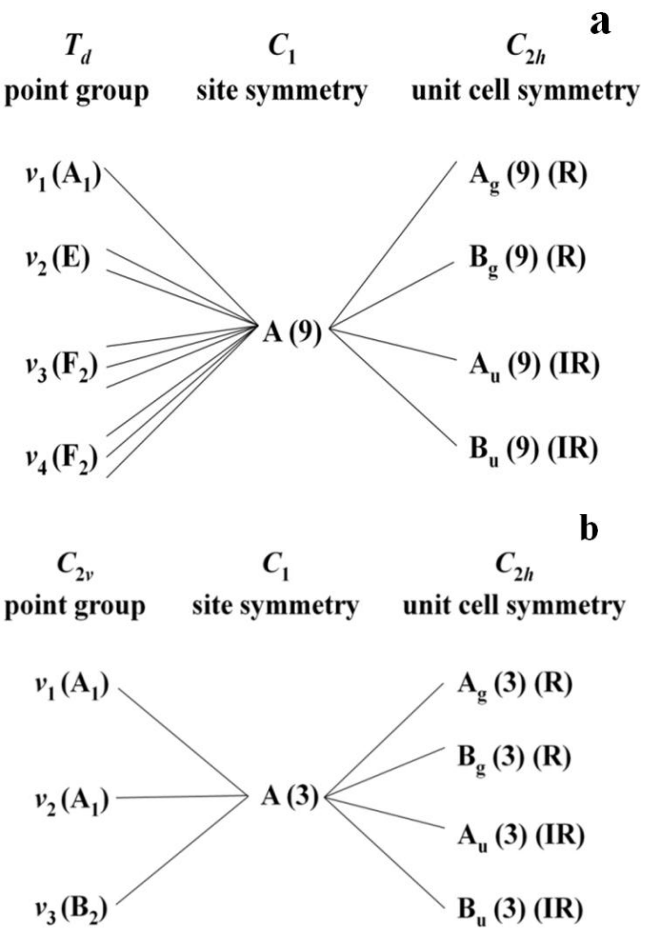

Figure 3: Correlation diagrams between: (a) T_d point symmetry, C_1 site symmetry and C_{2h} factor group symmetry (SO_4^{2-} ions); (b) C_{2v} point symmetry, C_1 site symmetry and C_{2h} factor group symmetry (water molecules)

The 114 vibrational modes of the unit cell decompose, as follows:

Γ = 27Ag + 27Bg + 30Au + 30Bu; where 1Au + 2Bu are translations (acoustic modes).

Since the crystal structures of the blödite- and kröhnkite-type compounds are centrosymmetric, the Raman modes display g-symmetry, and their IR counterparts display u-symmetry (mutual exclusion principle).

According to the site symmetry analysis the SO_4^{2-} ions in both compounds $Na_2Cu(SO_4)_2{\cdot}2H_2O$ and $Na_2Zn(SO_4)_2{\cdot}4H_2O$ are expected to exhibit three bands corresponding to the asymmetric modes ν_3 and ν_4, two bands for ν_2 (the SO_4^{2-} ions in C_1 site symmetry). The ν_1 is activated (all species of A symmetry). The factor group symmetry predicts splitting of each mode into four components – A_g + B_g + A_u + B_u. Fig. 3 shows the correlation between T_d

point symmetry, C_1 site symmetry and C_{2h} factor group symmetry (Fig. 3a) and C_{2v} point symmetry, C_1 site symmetry and C_{2h} factor group symmetry (Fig. 3b).

2) Vibrational spectra of the neat sulfates and $Na_2Zn_{1-x}Cu_x(SO_4)_2{\cdot}4H_2O$ solid solutions:

Vibrations of the tetrahedral ions

The data concerning vibrational spectra of the sodium zinc tetrahydrate and sodium copper sulfate dihydrate are scanty. As was mentioned above in the Introduction the hydrogen bonding system in the blödite-type compounds $Na_2M(SO_4)_2{\cdot}4H_2O$ (M = Mg, Co, Ni, Zn) is discussed in a previous paper of one of the authors [8]. No data for the vibrational behavior of the sulfate ions in $Na_2Zn(SO_4)_2{\cdot}4H_2O$ have been found. Raman and infrared spectra of $Na_2Cu(SO_4)_2{\cdot}2H_2O$ are discussed in Refs. [18-20]. Factor group analysis of the sodium copper sulfate dihydrate is briefly commented in Ref. [19]. The strength of the hydrogen bonds in the copper compound as deduced from the wavenumbers of ν_{OD} of HDO molecules (method of isotopic dilution) is reported in Ref. [12].

Infrared spectra of the neat compounds and the $Na_2Zn_{1-x}Cu_x(SO_4)_2{\cdot}4H_2O$ (x = 0.5, 0.09 and 0.14) solid solutions are presented in Fig. 4. Raman spectra of the neat compounds are shown in Fig. 5 (see also Table 2).

The sulfate ions in $Na_2Zn(SO_4)_2{\cdot}4H_2O$ display two infrared bands centered at 1153 and 1107 cm^{-1} corresponding to site symmetry components of ν_3. The band of small intensity at 987 cm^{-1} arises from the symmetric stretches of the sulfate ions. The appearance of two infrared bands only for ν_3 instead of three bands expected as deduced from the site symmetry analysis and one band for ν_1 shows that the local molecular symmetry of these ions is close to C_{3v} – *effective* spectroscopic symmetry (at least at ambient temperature) (see Fig. 4a). This spectroscopic finding correlates with the slight geometric distortion of the sulfate tetrahedra in $Na_2Zn(SO_4)_2{\cdot}4H_2O$ (Δr has a value of 0.027 Å; Δr is the difference between the longest and the shortest S–O bond distances in the sulfate tetrahedra [8]. However, the Raman spectrum shows that the ν_3 modes appear in a broader spectral range as compared to those in the IR spectrum – four bands at 1190, 1160, 1101 and 1067 cm^{-1}, thus indicating the influence of the crystal field effect on the numbers of the Raman bands (ν_3 splitting have values of 46 and 123 cm^{-1} for the infrared and Raman bands, respectively; see Fig. 5).

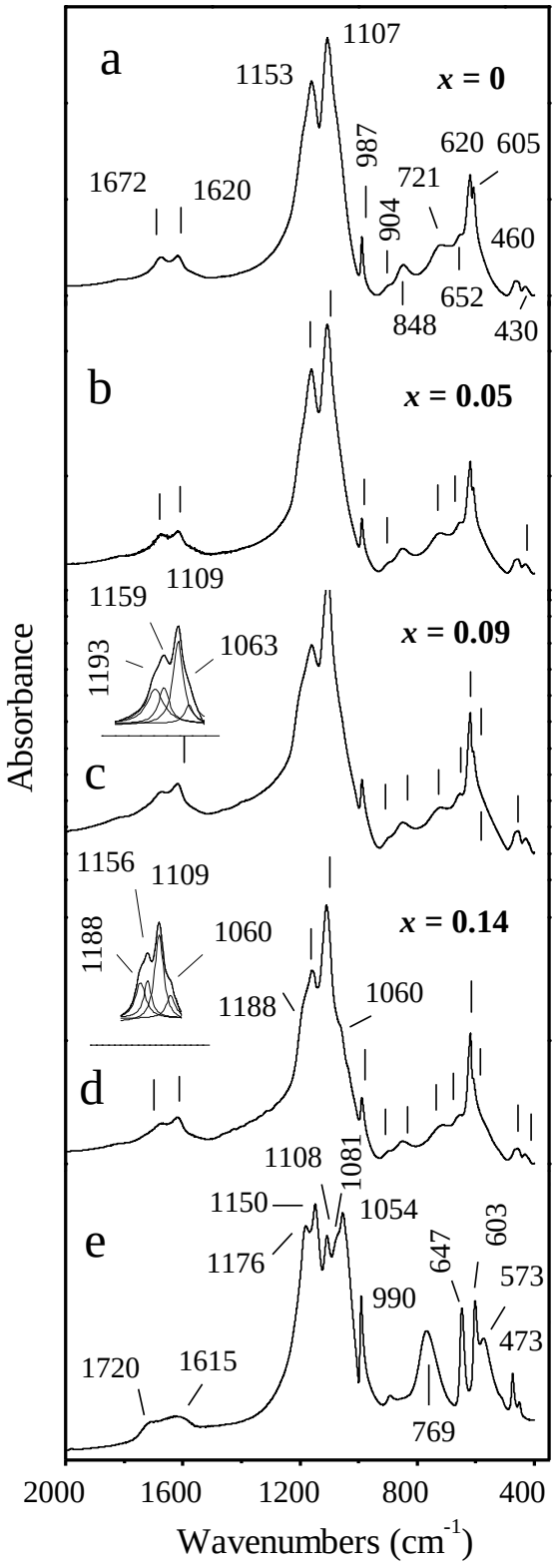

Figure 4: Infrared spectra in the region of the normal vibrations of the sulfate ions, the bending modes of the water molecules and water librations (a, $Na_2Zn(SO_4)_2{\cdot}4H_2O$; b, c, d, $Na_2Zn_{1-x}Cu_x(SO_4)_2{\cdot}4H_2O$; e, $Na_2Cu(SO_4)_2{\cdot}2H_2O$)

TABLE II

ASSIGNMENTS OF THE IR AND RAMAN BANDS TO VIBRATIONAL MODES IN THE REGION OF 1700–400 CM^{-1} (NORMAL VIBRATIONS OF THE SULFATE TETRAHEDRA, BENDING MODES OF WATER MOLECULES, WATER LIBRATIONS)

Vibrational mode	**$Na_2Zn(SO_4)_2·4H_2O$**		**$Na_2Cu(SO_4)_2·2H_2O$**	
	IR	**Raman**	**IR**	**Raman**
$\nu_2(H_2O)$	1672 1620		1615	
$\nu_3(SO_4)$	1153 1107	1190 1160 1101 1067	1179 1150 1108 1081 1054	1178 1162 1154 1135 1048
$\nu_1(SO_4)$	987	989	990	992 984
$L_R(H_2O)$	898		769	
	848			
$L_W(H_2O)$	721		573	
	652			
$\nu_4(SO_4)$	620 605	615	647 603	658 613
$\nu_2(SO_4)$	460 430	473 451	473 452	462 447

The asymmetric stretching modes ν_3 of the sulfate ions in $Na_2Cu(SO_4)_2·2H_2O$ appear in a wide spectral range of 125 cm^{-1} (splitting of ν_3) – bands at 1176, 1150, 1108, 1081 and 1054 cm^{-1} (see Fig. 4e).

The Raman bands corresponding to ν_3 are detected at 1178, 1162, 1154, 1135 and 1048 cm^{-1} (the splitting of ν_3 has value of 130 cm^{-1}; see Fig. 5b). Thus, the comparison of the infrared spectra of the zinc and copper compound indicate that stronger interaction between the identical sulfate oscillators occurs in the structure of the latter compound. The different vibrational behavior of the sulfate ions in both compounds is due probably to several factors: (i) the different arrangement of the polyhedra in both structures; (ii) the comparatively large differences in the unit cell volumes (384.91 and 498.8 Å for the copper and zinc salt, respectively); (iii) the different coordination environment of the metal(II) ions; (iv) the different NaO_x polyhedra in both compounds (NaO_6 in $Na_2Zn(SO_4)_2·4H_2O$ and NaO_7 in $Na_2Cu(SO_4)_2·2H_2O$).

As far as the intensity of the bands corresponding to the symmetric stretches ν_1 are concerned the infrared spectroscopic measurements reveal that this band in the spectrum of the copper compound is much more intensive than the respective band in the zinc compound. According to Petruševski and Šoptrajanov the intensities of the bands corresponding to ν_1 reflect the degree of distortion of the sulfate ions in a series of salts – the higher the intensity of these bands is the stronger the geometric distortion of the polyatomic ions is [21]. Indeed, Δr for the sulfate tetrahedra in the copper compound is slightly larger than that for the same ions in the zinc one (0.037 and 0.027 Å, respectively). However, the very high intensity of the band corresponding to ν_1 in the spectrum of the copper compound could not be explained with this small difference in the extent of geometric distortion of the sulfate tetrahedra in both compounds. In our opinion, the impact of the band positions on their intensities has to be taken into considerations additionally to the values of Δr. For example, our spectroscopic studies on Tutton selenates, $Rb_2M(SeO_4)_2·6H_2O$ and $Cs_2M(SeO_4)_2·6H_2O$ (M = Mg, Co, Ni, Zn) show that some coupling between ν_1 and ν_3 of the selenate ions occurs and as a result the intensities of the infrared bands corresponding to ν_1 increase considerably as expected if only the geometric distortion of these ions are concerned [22, 23]. Indeed, the differences in the wavenumbers of the bands corresponding to the lowest wavenumbered component of ν_3 and ν_1 for the zinc compound has a value of 120 cm^{-1}, while that for the copper one is 64 cm^{-1}, i.e. this difference plays a considerable role on

the intensity of the band at 990 cm^{-1} in the spectrum of $Na_2Cu(SO_4)_2{\cdot}2H_2O$ (compare Fig. 4a and e). The Raman band at 989 cm^{-1} is attributed to ν_1 of the sulfate ions in the zinc compound and those at 992 and 984 cm^{-1} to ν_1 of the sulfate ions in the copper one (the appearance of two bands for ν_1 in the Raman spectrum of the copper compound is owing to the crystal field effect).

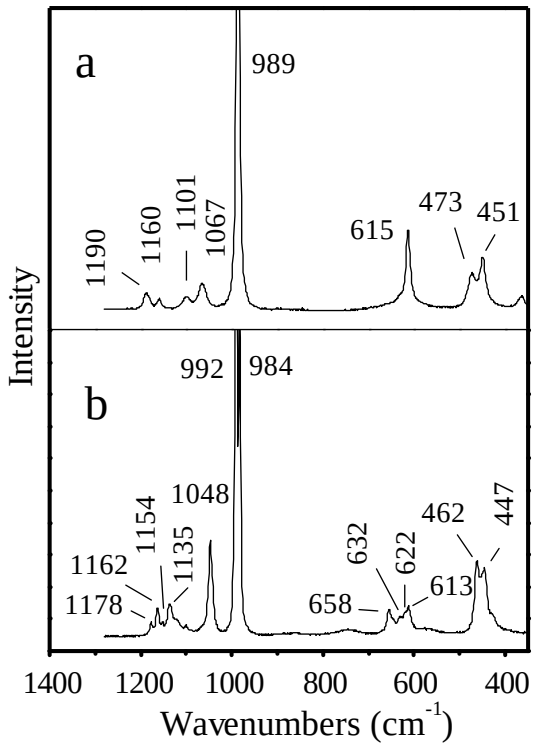

Figure 5 : Raman spectra in the region of the normal vibrations of the sulfate ions (a, $Na_2Zn(SO_4)_2{\cdot}4H_2O$; b, $Na_2Cu(SO_4)_2{\cdot}2H_2O$)

The infrared bands at 620 and 605 cm^{-1}, and those to 647 and 603 cm^{-1} originate from the asymmetric bending motions ν_4 in the zinc and copper compounds, respectively (the Raman bands appear at 615 cm^{-1}, and 658, 632, 622 and 613 cm^{-1} for the zinc and copper salts, respectively; see Fig. 5). The infrared bands at lower frequencies 460 and 430 cm^{-1} (zinc compound), and 473 and 453 cm^{-1} (copper compound) are assigned to two site symmetry components of ν_2. The Raman bands corresponding to ν_2 are observed at 473 and 451 cm^{-1} (zinc compound), and 462 and 447 cm^{-1} (copper compound). The larger values of ν_4 splitting for the copper salt than that for the zinc one indicate that the sulfate tetrahedra in the former are stronger distorted with respect to the corresponding bond angles O–S–O (44 and 15 cm^{-1} for the copper and zinc compounds, respectively, (infrared spectra) and 45 cm^{-1} (Raman spectrum of the copper compound) in agreement with the structural data [8].

Additionally, it is important to notice that the IR and Raman bands differ in the wavenumbers in agreement with the group theoretical analysis (see Table 2). Considering the highest frequency Raman band in the spectrum of the zinc compound the value of the g–u splitting is 37 cm^{-1} (1153 cm^{-1} (IR) and 1190 cm^{-1} (Raman)) and considering the lowest frequency infrared band the value of u–g splitting is 40 cm^{-1} (1107 cm^{-1} (IR) and 1067 cm^{-1} (Raman)). The data in the Table 2 show that the splitting of g–u modes has values of about 10 cm^{-1} as far as the ν_4 and ν_2 modes are concerned.

The inclusion of the copper ions in the crystals of the zinc compound up to 9 mol% does not change the shape of the spectra in the region of ν_3. In the spectrum of the sample $Na_2Zn_{0.91}Cu_{0.09}(SO_4)_2{\cdot}4H_2O$ two shoulders at 1193 and 1063 cm^{-1} appear, which are attributed to ν_3 of the sulfate ions forming new bonds of the type $Cu–OSO_3$.

Vibrations of the water molecules in the neat sulfates

Spectra of $Na_2Zn(SO_4)_2{\cdot}4H_2O$ and $Na_2Cu(SO_4)_2{\cdot}2H_2O$ in the region of ν_{OH} and ν_{OD} are shown in Fig. 6 (the spectra in the region of ν_{OD} are taken from Refs. [8, 12]).

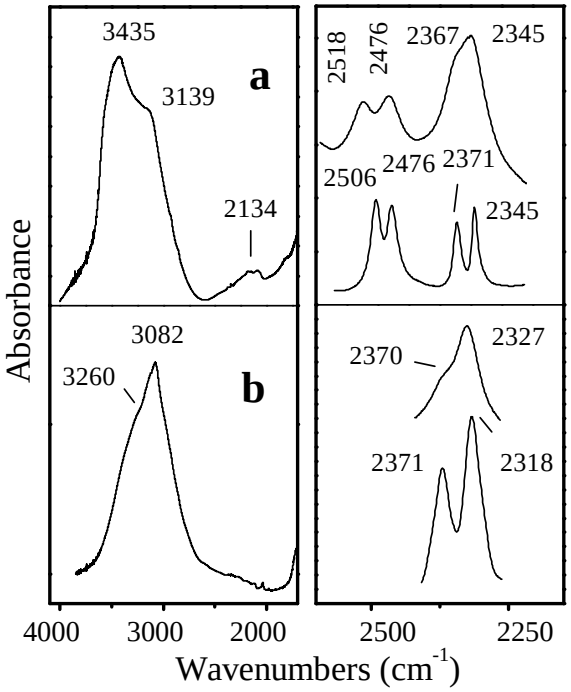

Figure 6: Infrared spectra in the region of ν_{OH} and ν_{OD} of matrix-isolated HDO molecules (a, $Na_2Zn(SO_4)_2{\cdot}4H_2O$; b, $Na_2Cu(SO_4)_2{\cdot}2H_2O$; the spectra at liquid nitrogen temperature are taken from Refs, [9,13])

The two crystallographically different water molecules in the structure of $Na_2Zn(SO_4)_2{\cdot}4H_2O$ form four Ow···O bonds, as follows: Ow1···O1 = 2.704 Å; Ow1···O4 = 2.745 Å; Ow2···O1 = 2.868; Ow2···O4 = 2.926 Å. According to the site symmetry analysis (water molecules in C_1 site symmetry) four bands corresponding to ν_{as} and ν_s of water are expected to appear in the spectrum of the zinc compound in high frequency region. However, instead of four bands expected two bands only at 3435 and 3139 cm^{-1} are seen in the spectrum (Fig. 6a) due to the interactions of identical oscillators. As is expected the matrix-isolated HDO molecules in the structure of the zinc compound exhibit four bands, thus indicating the formation of four hydrogen bonds of different strength. The bands at 2506 and 2476 cm^{-1} correspond to water molecules Ow2 linked to the zinc ions via the longest bond (bonds Ow2–Zn are 2.132 Å) and the bands at 2371 and 2345 cm^{-1} correspond to those linked to the zinc ions via the shortest ones (bonds Ow1–Zn are 2.065 Å; spectra at liquid nitrogen temperature). Consequently, the band at higher frequency 3435 cm^{-1} is attributed to Ow2 and that at 3139 cm^{-1} to Ow1. The isotopic ratios have values of 1.37 and 1.39 for Ow2 and 1.32 and 1.34 for Ow1. The spectroscopic experiments show that the water molecules are energetically distorted – $\Delta\nu$ is 30 cm^{-1} for Ow2 and 26 cm^{-1} for Ow1. The copper compound displays two bands in the high frequency region – at 3260 and 3082 cm^{-1}, which are assigned to ν_{as} and ν_s of the water molecules (one structural type in C_1 site symmetry). The ν_{OD} modes appear at 2370 and 2327 cm^{-1} ($\Delta\nu$ = 43 cm^{-1}; Ow···O bond distances are 2.696 and 2.626 Å, respectively; spectra at liquid nitrogen temperature; see Fig. 6b). The isotopic ratios have values of 1.37 and 1.32.

The bands at 1672 and 1620 cm^{-1} are assigned to bending modes of the two crystallographically different water molecules in the zinc compound (see Fig. 4a). The comparatively large difference in the frequencies for ν_2 ($\Delta\nu$ = 52 cm^{-1}) is due to the structural difference of the water molecules as was commented above in the text. The band at 1615 cm^{-1} (Fig. 4e) originates from the bending modes of the water molecules coordinated to the copper ions. The band at the larger frequency (1720 cm^{-1}) is due to vibrational interactions between the bending modes ν_2 and overtones or combinations of water librations.

The water librations (rocking, twisting and wagging) are observed in the spectral region bellow 1000 cm^{-1} and some coupling with vibrations of other species occurs (see Fig. 4). Each type of water molecules in the sulfates under study will exhibit two bands for the rocking and wagging modes, respectively (twisting modes (species of symmetry A_2) are not active in the infrared spectra in the case when the symmetry of the water molecules do not deviate considerably from C_{2v} [21]).The assignments of the bands are made by analogy to the respective water librations in Tutton compounds, $M'M''(XO_4)_2{\cdot}6H_2O$ (M' = K, Rb, Cs; M'' = Mg, Co, Ni, Cu, Zn; X= S, Se) [22, 23, 26-28]. According to the considerations made in these papers water molecules linked to the metal(II) ions via the shorter bonds are much more polarized than those linked via the longer bonds due to the stronger *synergetic* effect of the metal ions and consequently the water librations for the former molecules occur at higher frequencies. On the other hand, the rocking modes appear at larger wavenumbers as compared to the wagging ones. The weak bands at 904, 848, 721 and 652 cm^{-1} in the spectrum of $Na_2Zn(SO_4)_2{\cdot}4H_2O$ are assigned to water librations. Thus, we assign the bands at 904 and 721 cm^{-1} to the rocking and wagging motions of Ow1, and those at 848 and 652 cm^{-1} to the respective motions of Ow2 (Fig. 4a). It is reported in the literature that the splitting of the bands corresponding to the wagging modes is a measure for the deformation of the octahedral hydrate sphere. Indeed, the data for Tutton selenates presented in Ref. [26] show that with exception of two copper Tutton compounds the values of ΔL_W are not more than 60 cm^{-1}. In the case of $Na_2Zn(SO_4)_2{\cdot}4H_2O$ ΔL_W has a value of 69 cm^{-1} in agreement with the structural data. The bands at 769 cm^{-1} and 573 cm^{-1} in the spectrum of $Na_2Cu(SO_4)_2{\cdot}2H_2O$ originate from the rocking and wagging modes, respectively. The intensity of the band at 573 cm^{-1} is unusually high for this kind of water motions and in our opinion this fact is owing to strong interactions between the wagging vibrations and the bending modes of the sulfate tetrahedra (see Fig. 4e).

C. EPR spectra of the neat sulfates and the $Na_2Zn_{0.86}Cu_{0.14}(SO_4)_2{\cdot}4H_2O$ solid solution

Fig. 7 shows the EPR spectra of Cu^{2+} ions stabilized in the blödite-type structure (the copper content being varied from 2 to 14 mol%). At room temperature, all spectra consist of axially symmetric signal with $g_\perp$ =

2.30 and $g_{||}$ = 2.03. Although the g-values are constants, the relative intensity of the EPR signal increases followed the copper content in the solid solutions $Na_2Zn_{1-x}Cu_x(SO_4)_2 \cdot 4H_2O$: I_{EPR} = 1.0, 2.4 and 7.0 for x = 0.02, 0.05 and 0.14, respectively. This indicates that Cu^{2+} ions gives rise to the EPR profile. By lowering the temperature from 290 to 100 K, both the perpendicular and parallel components of the *g*-tensor are split into several lines due to the coupling between electron and nuclear spins of Cu^{2+} ions (Fig. 7b). The structured spectrum is simulated taking into account the *g*-anisotropy and hyperfine interaction for Cu^{2+} ions. The calculated EPR parameters comprising the g-tensor and the hyperfine constant are listed on Table 3. For the sake of comparison, the previously reported EPR data on Cu^{2+} ions doped $Na_2Zn(SO_4)_2 \cdot 4H_2O$ are also given [29, 30]. Two important features can be underlined. First, both the *g*-tensor and the hyperfine constant, *A*, are insensitive towards the copper content. The calculated *g*- and *A*-values are close to those previously published for copper containing $Na_2Zn(SO_4)_2 \cdot 4H_2O$ [29, 30]. The only parameter that depends on the coper content is the EPR line width: there is a progressive line broadening by increasing the total copper content. For the solid solutions containing the highest copper amount (i.e. x = 0.14), the line width is too large that prevent the observation of the fine structure (Fig. 7). These observations demonstrate clearly that all Cu^{2+} ions are detected by EPR and they are included in the blödite structural matrix by forming solid solutions. Second, the *g*-tensor undergoes at lower temperature a change from axially symmetric to orthorhombic. In the same order, the hyperfine structure becomes clearly resolved for all components of the low-temperature *g*-tensor. This means that, at low temperature, Cu^{2+} ions are in orthorhombically distorted crystal sites, while on heating the symmetry is averaged into axially symmetric one. The observed EPR feature can be explained with cooperative Jahn-Teller interactions between Cu^{2+} ions. In the blödite-type of structure, there are distinct structural motives of Cu^{2+} ions coordinated by four water molecules and two sulfate ions, thus forming $[Cu(H_2O)_4(SO_4)_2]^{2-}$ clusters, which are tilted one to another in opposite directions. The short and long Cu–O bonds of adjacent $[Cu(H_2O)_4(SO_4)_2]^{2-}$ clusters are arranged in a proper manner, that produce additional lattice strains around a given center. These interactions take place via the hydrogen bond network, which are strongly temperature dependent. It appears that cooperative Jahn-Teller effect stabilizes at low temperature the orthorhombic symmetry of $[Cu(H_2O)_4(SO_4)_2]^{2-}$ ions.

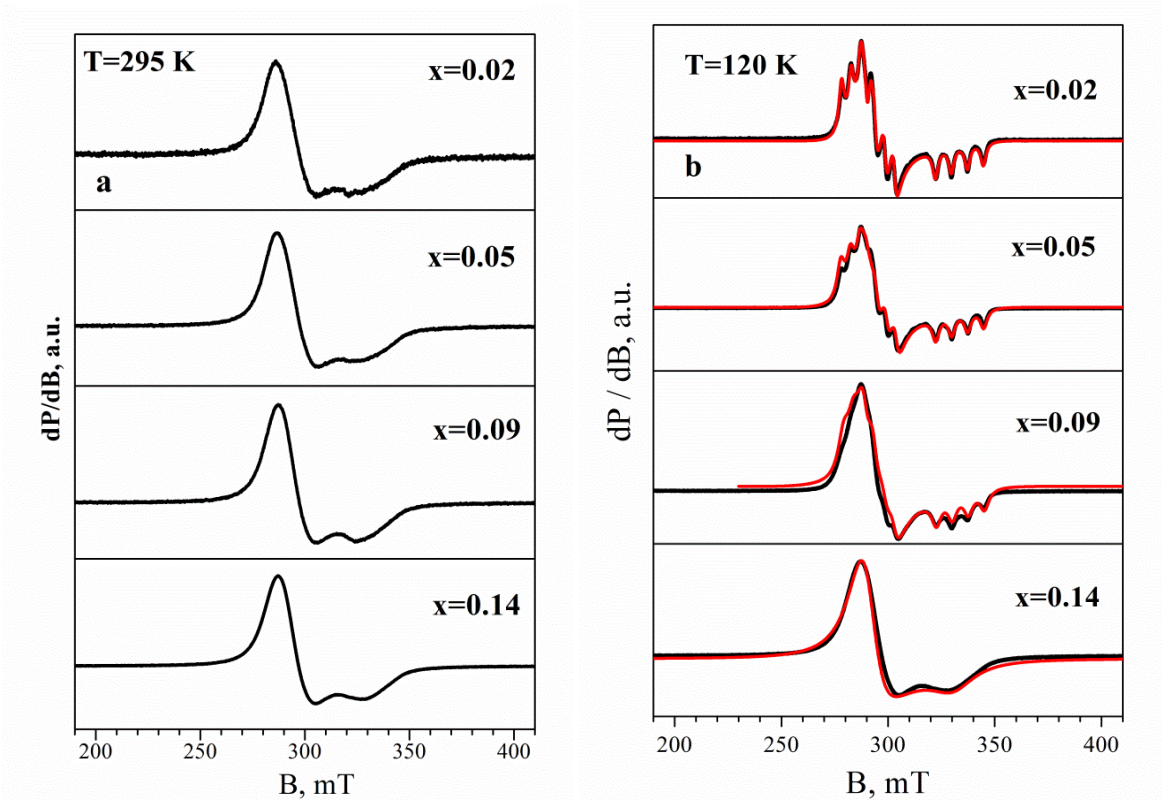

Figure 7: EPR spectra at 295 and 120 K of $Na_2Zn_{1-x}Cu_x(SO_4)_2 \cdot 4H_2O$ (x = 0.02, 0.05, 0.09 and 0.14). The experimental and simulated spectra are indicated with black and red lines, respectively

It is interesting to note that the same EPR picture has been observed for the copper(II) Tutton's salts, $X_2[Cu(H_2O)_6](YO_4)_2$, where isolated $[Cu(H_2O)_6]^{2+}$ complexes appears [31]. These salts have been described as model systems, in which the geometry adopted by $[Cu(H_2O)_6]^{2+}$ octahedra is a result from the interplay of the Jahn-Teller vibronic coupling and crystal lattice [32].

The EPR spectra of Cu^{2+} ions in $Na_2Cu(SO_4)_2{\cdot}2H_2O$ are presented on Fig. 8. As one can see, the EPR spectrum of Cu^{2+} ions in the kröhnkite-type phase is completely different in comparison with that for Cu^{2+} ions in the blödite-derived salts. Between 120 and 290 K, the EPR spectrum displays an axially symmetric signal having the g-values, for which $g_\perp < g_\parallel$ is fulfilling (Table 3). The same *g*-values have been already observed by Sarma *et al.* [33]. In addition, the hyperfine structure is not observed in the whole temperature range of 120-295 K. In comparison with the blödite-type salts, the EPR signal from Cu^{2+} ions in the kröhnkite-type phase is much broader (Table 3). Based on these EPR parameters, the axially symmetric signal can be assigned to Cu^{2+} ions in tetragonally elongated octahedral sites, which are coupled by magnetic exchange interactions. It appears that, in the kröhnkite structure, the geometry of the Cu^{2+} site is dominated by the Jahn-Teller effect. This is in opposite to what we observe for the blödite-type solid solutions. The other feature derived from EPR spectra of $Na_2Cu(SO_4)_2{\cdot}2H_2O$ obtained from solutions containing zinc ions is a lack of any effect of Zn^{2+} ions on the EPR parameters of Cu^{2+} ions: both the *g*-tensor and EPR line width are the same for all samples crystallized from solutions with different copper/zinc ratio. Thus, the EPR measurements are in agreement with the solubility diagram discussed above in the text (see Fig. 2), i.e. the Zn^{2+} ions are not included in the crystals of $Na_2Cu(SO_4)_2{\cdot}2H_2O$.

TABLE III

EПР PARAMETERS (G-TENSOR; HYPERFINE CONSTANT, A; LINE WIDTH, ΔH_{pp}) FOR Cu^{2+} IN BLÖDITE DERIVED SALTS, $Na_2Zn_{1-x}Cu_x(SO_4)_2{\cdot}4H_2O$ (x = 0.02, 0.05, 0.09 AND 0.14), AND KRÖHNKITE-TYPE $Na_2Cu(SO_4)_2{\cdot}2H_2O$. ALL EPR PARAMETERS ARE DETERMINED AT 120 K. FOR THE SAKE OF COMPARISON, THE PREVIOUSLY REPORTED EPR PARAMETERS ARE ALSO PROVIDED

	EPR parameters								
	g_1	g_2	g_3	A_1 mT	A_2 mT	A_3 mT	$\Delta H_{pp}^{\ 1}$ mT	$\Delta H_{pp}^{\ 2}$ mT	$\Delta H_{pp}^{\ 3}$ mT
x = 0.02	2.367	2.276	2.0231	4.5	4.5	7.5	1.8	1.8	1.8
x = 0.05	2.37	2.277	2.0221	4.5	4.5	7.5	2.5	2.5	2.3
x = 0.09	2.359	2.278	2.0201	4.3	4.7	7.6	3.5	3.5	3.0
x = 0.14	2.3184	2.3184	2.039	-	-	-	11.0	11.0	15.0
Cu^{2+} in $Na_2Zn(SO_4)_2{\cdot}4H_2O$ [29]	2.350	2.142	2.035	7.0	0.7	9.4	-	-	-
Cu^{2+} in $Na_2Zn(SO_4)_2{\cdot}4H_2O$ [30]	2.3472	2.2356	2.0267	9.41	2.89	5.78	-	-	-
Cu^{2+} in $Na_2Cu(SO_4)_2{\cdot}2H_2O$	2.3855	2.119	2.100	-	-	-	45	35	35
Cu^{2+} in $Na_2Cu(SO_4)_2{\cdot}2H_2O$ [33]	2.339	2.085	2.096	-	-	-	-	-	-

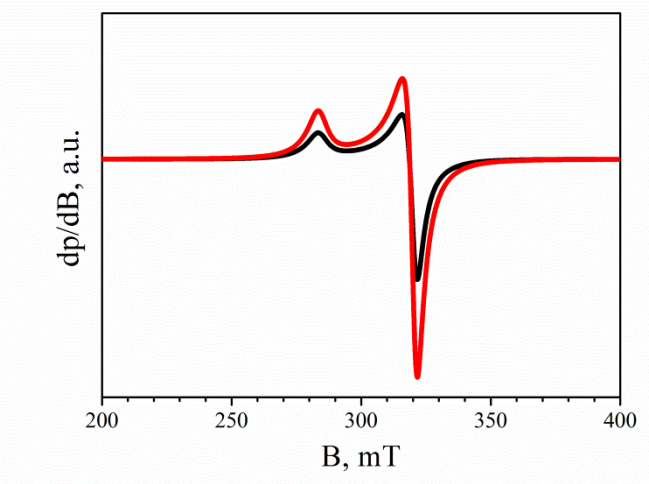

Figure 8: EPR spectra of Cu^{2+} in the neat kröhnkite-type $Na_2Cu(SO_4)_2{\cdot}2H_2O$ (red) and in $Na_2Cu(SO_4)_2$ $2H_2O$ obtained from solutions with different copper/zinc ratio (black)

IV. CONCLUSION

Solid solutions $Na_2Zn_{1-x}Cu_x(SO_4)_2{\cdot}4H_2O$ ($0 > x < 0.14$; blödite- type structure) and sodium copper kröhnkite $Na_2Cu(SO_4)_2{\cdot}2H_2O$ crystallize from mixed sodium zinc copper solutions. The zinc ions do not include in the crystals of $Na_2Cu(SO_4)_2{\cdot}2H_2O$, i.e. they do not accept the coordination environment of the copper ions in the strongly distorted CuO_6 octahedra.

The different vibrational behavior of the SO_4^{2-} ions in $Na_2Zn(SO_4)_2{\cdot}4H_2O$ and $Na_2Cu(SO_4)_2{\cdot}2H_2O$ is probably due to the comparatively large differences in the unit cell volumes of both compounds, the different coordination environment of the metal(II) ions and the different composition of the NaO_x polyhedra. The sulfate tetrahedron in $Na_2Zn(SO_4)_2{\cdot}4H_2O$ exhibits a molecular symmetry higher than the crystallographic one (*effective* spectroscopic symmetry C_{3v}). The hydrogen bond strength in $Na_2Cu(SO_4)_2{\cdot}2H_2O$ is stronger than that in $Na_2Zn(SO_4)_2{\cdot}4H_2O$ as deduce from the wavenumbers of the ν_{OD} modes of matrix-isolated HDO molecules due to the stronger *synergetic* effect of the copper ions as compared to the zinc ions.

EPR measurements reveal that at low temperature the Cu^{2+} ions in the solid solutions are in orthorhombically distorted crystal sites, while on heating the symmetry is averaged into axially symmetric one. The Cu^{2+} ions in $Na_2Cu(SO_4)_2{\cdot}2H_2O$ are in tetragonally elongated octahedral sites, which are coupled by magnetic exchange interactions.

V. Acknowledgements

The financial support from the Scientific Research Department of the University of Chemical Technology and Metallurgy (Republic of Bulgaria) is acknowledged (Project No 11603/2016).

VI. REFERENCES

[1] Reynaud, M., Ati, M., Boulineau, S., Sougrati. M. T., Melot, B. C., Rousse, G., Chotard, J. N., and Tarascon, J. M. 2013. Bimetallic Sulfates $A_2M(SO_4)_2{\cdot}nH_2O$ (A = Li, Na and M = Transition Metal): as New Attractive Electrode Materials for Li- and Na-Ion Batteries. ECS Transactions, 50, 11-19, Print ISSN: 1938-6737; Online ISSN: 1938-5862, DOI: 10.1149/05024.0011ecst.

[2] Reynaud, M., 2013, Design of new sulfate-based positive electrode materials for Li- and Na-ion batteries. Material chemistry. Université de Picardie Jules Verne, France, English version.

[3] Marinova, D., Kostov, V., Nikolova, R., Kukeva, R., Zhecheva, E., Sendova-Vasileva, M., and Stoyanova, R. 2015. From kröhnkite- to alluaudite-type of structure: novel method of synthesis of sodium manganese sulfates with electrochemical properties in alkali-metal ion batteries. J. Mater. Chem., A3, 22287–22299, ISSN 2050-7488, DOI: 10.1039/C5TA07204B.

[4] Giglio, M. 1958. Die Kristallstruktur von $Na_2Zn(SO_4)_2.4H_2O$ (Zn-Blödit). Acta Crystallogr., 11, 789-794, ISSN: 0365-110X, DOI: 10.1107/S0365110X5800222X.

[5] Bukin, V. I., and Nozik, Yu. Z. 1974. A neutronographic investigation of hydrogen bonding in zinc astrakanite $Na_2Zn(SO_4)_2{\cdot}4H_2O$. J. Struct. Chem., 15, 616–619, Print ISSN 0022-4766; Online ISSN 1573-8779, DOI: 10.1007/BF00747212.

[6] Hawthorne, F. C. 1985. Refinement of the crystal structure of bloedite; structural similarities in the [VIM(IVTPhi4)2Phin) finite-cluster minerals. Can. Mineral., 23, 669–674, Print ISSN: 0008-4476; Online ISSN: 1499-1276.

[7] Vizcayno, C., and Garcia-Gonzalez, M. 1999. $Na_2Mg(SO_4)_2.4H_2O$, the Mg and-member of the bloedite-type of mineral. Acta Crystallogr.: Cryst.

Struct. Commun., C55, 8–11, ISSN: 2053-2296, DOI: 10.1107/S0108270198011135.

[8] Stoilova, D., and Wildner, M. 2004. Blödite-type compounds $Na_2Me(SO_4)_2{\cdot}4H_2O$ (Me = Mg, Co, Ni, Zn): crystal structure and hydrogen bonding systems. J. Mol. Struct., 706, 57-63, ISSN: 0022-2860, DOI:10.1016/j.molstruct.2004.01.070.

[9] Fleck, M., Kolitsch, U., and Hertweck, B. 2002. Natural and synthetic compounds with kröhnkite-type chains: review and classification, Z. Kristallogr., NCS, 217, 1-9, Online ISSN 2196-7105, DOI: 10.1524/zkri.217.9.435.22883.

[10] Fleck, M., and Kolitsch, U. 2003. Natural and synthetic compounds with krohnkite-type chains. An update. Z. Kristallogr., NCS, 218, 553-567, ISSN 2196-7105, DOI: 10.1524/zkri.218.8.553.20689.

[11] Hawthorne, F. C., and Ferguson, R. B. 1975. Refinement of the crystal structure of Kroehnkite. Acta Crystallogr., B31, 1753-1755, ISSN: 2052-5206, DOI: 10.1107/S0567740875006048.

[12] Stoilova, D., Wildner, M., and Koleva, V. 2002. Infared study of ν_{OD} mods in isotopically dilute (HDO molecules) $Na_2Me(XO_4)_2{\cdot}2H_2O$ with matrix-isolated $X'O_4^{2-}$ guest ions (Me = Mn, Co, Ni, Cu, Zn, Cd; X – S, Se). J. Mol. Struct., 643, 37-41, ISSN: 0022-2860, DOI: 10.1016/S0022-2860(02)00404-0.

[13] Ternary and Polycomponent Systems of Inorganic Compounds, Izd. Nauka, Leningrad, 3 (1970) 1010, 1012.

[14] Balarew, Chr., Karaivanova, V, and T. Oikova, T. 1970. Contribution to the study of the isomorphic and isodimorphic inclusions in crystal salts. III. Examination of the systems zinc sulfate-cobalt sulfate-water and zinc sulfate water- nickel sulfate-water at 25°C. Chem. Commun. Departm. Bulg. Acad. Sci., 3, 673-644.

[15] Trendafelov, D., and Balarew, Chr. 1968. Beitrag sur Untersuchung der isomorphen und isodimorphen Einschlusse in Kristallsalzen. II. Untersuchung der Verteiligung der Kobaltionen in verschiedenen Zinksulfathydraten. Comm. Dept. Chem. Bulg. Acad. Sci. 1 (1968) 73-80.

[16] Balarew, Chr., and Karaivanova, V. 1975. Change in the Crystal Structure of Zink(II) Sulphate Heptahydrate and Magnesium Sulphate Heptahydrate Due to Isodimorphous Substitution by Copper(II), Iron(II) and Cobalt(II) Ions. Krist. Technik. 10, 1101-1110.

[17] Nakamoto, K. Infrared and Raman spectra of Inorganic and Coordination Compounds, John Wiley & Sons, New York, 1986.

[18] Stoilova, D., Wildner, M., and Koleva, V. 2003. Vibrational behavior of the S–O stretches in compounds with kröhnkite-type chains $Na_2Me(SeO_4)_2{\cdot}2H_2O$ with matrix-isolated SO_4^{2-} and M'^{2+} guest ions (Me= Mn, Co, Ni, Cu, Zn, Cd). Vib. Spectrosc., 31, 115-123, ISSN: 0924-2031, DOI: 10.1016/S0924-2031(02)00104-2.

[19] Mahadevan Pillai, V. P., Nayar, V. U., and Jordanovska, V.B. 1997. Infrared and Raman Spectra of $Na_2Cu(SO_4)_2{\cdot}2H_2O$ and $(CH_3NH_3)_2M(II)(SO_4)_2{\cdot}6H_2O$ with M(II)=Cu, Zn, and Ni. J. Solid State Chem., 133, 407-415, ISSN: 0022-4596, DOI: 10.1006/jssc.1997.7486.

[20] Frost, R. L., Hi, Y., and Scholz, R. 2013. Vibrational Spectroscopy of the Copper (II) Disodium Sulphate Dihydrate Mineral Kröhnkite $Na_2Cu(SO_4)_2{\cdot}2H_2O$. Spectrosc. Lett., 46, 447-452, Print ISSN: 0038-7010; Online ISSN: 1532-2289, DOI: 10.1080/00387010.2012.753906

[21] Petruševski, V., and Šoptrajanov, B. 1988. Description of molecular distortions. II. Intensities of molecular distortions II. Intensities of the symmetric stretching bands of tetrahedral molecules. J. Mol. Struct., 175, 349-354, ISSN: 0022-2860, DOI: 10.1016/S0022-2860(98)80101-4

[22] Karadjova, V., Kovacheva, D., and Stoilova, D. 2014. Study on the cesium Tutton compounds, $Cs_2M(XO_4)_2{\cdot}6H_2O$ (M = Mg, Co, Zn; X = S, Se): Preparation, X-ray powder diffraction and infrared spectra. Vib. Spectrosc., 75, 51-58, ISSN: 0924-2031, DOI: 10.1016/j.vibspec.2014.09.006.

[23] Karadjova, V., and Stoilova, D. 2013. Infrared spectroscopic study of $Rb_2M(XO_4)_2{\cdot}2H_2O$ (M = Mg, Co, Ni, Cu, Zn; X = S, Se) and of SO_4^{2-} guest ions included in rubidium Tutton selenates. J. Mol. Struct., 1050, 204-210, ISSN: 0022-2860, DOI: 10.1016/j.molstruc.2013.07.013

[24] Eriksson, A., Lindgren, J. 1978. Model calculations of the vibrations of bonded water molecules. J. Mol. Struct., 48, 417-430, ISSN: 0022-2860, DOI: 10.1016/0022-2860(78)87252-4.

[25] Campbell, J. A., Ryan, D. P., and Simpson, L.M. 1970. Interionic forces in crystal-II. Infrared spectra of SO_4 groups and 'octahedrally' coordinated water in some alums, Tutton salts, and the double salts obtained by dehydrating them. Spectrochim Acta. 26A, 2351-2361, ISSN: 1386-1425, DOI: 10.1016/0584-8539(70)80188-X.

[26] Ebert, M., and Vojtísek, P. 1993. The hydrates of double selenates. Chem. Pap., 47, 292-296, Print ISSN: 0366-6352; Electron ISSN: 1336-9075.

[27] Mička, Zd., Prokopová, L., Cisařová, I., and Havliček, D. 1996. Crystal structure, thermoanalytical properties and infrared spectra of double magnesium selenates. Collect. Czech. Chem. Commun., 61, 1295-1306, Printed ISSN 0010-0765, Electronic ISSN 1212-6950, DOI: 10.1135/cccc19961295.

[28] Wildner, M., Marinova, D., and Stoilova, D. 2016. Vibrational spectra of $Cs_2Cu(SO_4)_2{\cdot}6H_2O$ and $Cs_2Cu(SeO_4)_2{\cdot}nH_2O$ (n=4, 6) with a crystal structure determination of the Tutton salt $Cs_2Cu(SO_4)_2{\cdot}6H_2O$. J. Mol. Struct., 1106, 440-451, ISSN: 0022-2860, DOI: 10.1016/j.molstruc.2015.11.008.

[29] Sastry, B. A., and Sastry, G. S. 1971. Electron spin resonance studies on Cu^{2+} doped $Na_2Zn(SO_4)_2.4H_2O$. J. Phys. C: Solid State Phys., 4, L347-L350, Print ISSN: 0022-3719, DOI: 10.1088/0022-3719/4/16/008.

[30] Kripal, R., and Shukla, S. 2011. EPR and Optical Study of Cu^{2+} Ions Doped in Sodium Zinc Sulfate Tetrahydrate Single Crystals. Appl. Magn. Reson., 41, 95-95, Print ISSN: 0937-9347; Online ISSN: 1613-7507, DOI: 10.1007/s00723-011-0246-0.

[31] Hitchman, M. A., Maaskant, W., van der Plas, J., Simmons, C. J., and Stratemeier, H. 1999. Cooperative Jahn−Teller Interactions in Dynamic Copper(II) Complexes. Temperature Dependence of the Crystal Structure and EPR Spectrum of Deuterated Ammonium Copper (II) Sulfate Hexahydrate. J. Am. Chem. Soc., 121, 1488-1501, Print Edition ISSN: 0002-7863; Web Edition ISSN: 1520-5126, DOI: 10.1021/ja981831w.

[32] Simmons, C., Stratemeier, H., Hitchman, M. A., and Riley, M. 2013. Influence of Lattice Interactions on the Jahn–Teller Distortion of the $[Cu(H_2O)_6]^{2+}$ Ion: Dependence of the Crystal Structure of $K_{2x}Rb_{2-2x}[Cu(H_2O)_6](SeO_4)_2$ upon the K/Rb Ratio. Inog. Chem., 52, 10481-10499, Print Edition ISSN: 0020-1669; Web Edition ISSN: 1520-510X DOI: 10.1021/ic401385f.

[33] Sarma, C. R. N., Satyanandam, G., Gopalakrishna Murthy, P. V., and Haranadh, C. 1976. EPR investigation of kröhnkite, $Na_2Cu(SO_4)_2{\cdot}2H_2O$. J. Phys. C: Solid State Phys., 9, 841-7, Print ISSN: 0022-3719, DOI: 10.1088/0022-3719/9/5/022.